Magnetic-field-induced multiple electronic states in $La_{0.5}Ca_{0.5}MnO_{3+\delta}$

Gang Xiao
Department of Physics, Brown University, Providence, Rhode Island 02912
and IBM T. J. Watson Research Center, Yorktown Heights, New York 10598

E. J. McNiff, Jr.
Francis Bitter National Magnet Laboratory, Massachusetts Institute of Technology, Cambridge, Massachusetts 02139

G. Q. Gong
Department of Physics, Brown University, Providence, Rhode Island 02912

A. Gupta
IBM T. J. Watson Research Center, Yorktown Heights, New York 10598

C. L. Canedy
Department of Physics, Brown University, Providence, Rhode Island 02912

J. Z. Sun
IBM T. J. Watson Research Center, Yorktown Heights, New York 10598
(Received 9 May 1996)

We have observed multiple electronic states in the presence of a magnetic field in the half-doped $La_{0.5}Ca_{0.5}MnO_{3+\delta}$ system. The resistivity of each state differs from one another by at least one order of magnitude. Application of a magnetic field induces first-order phase transitions among these states. A maximum 10^9-fold magnetoresistance ratio has been observed at 4.2 K between the least and the most conductive phases. Our results differ from early observations that there is only one metal-to-insulator (two states) transition in other related half-doped systems. [S0163-1829(96)06334-5]

In the perovskite manganate, $A_{1-x}B_xMnO_{3+\delta}$ (A=La, Pr, or Nd, B=Ca, Sr, or Ba), a strong interplay between lattice, magnetism, and transport brings out diverse types of magnetic orderings and magnetotransport properties.[1–11] The physics involved is both intriguing and complex. One needs to consider the superexchange in $Mn^{3+(4+)}$-O^{2-}-$Mn^{3+(4+)}$ and the Zener double exchange in Mn^{3+}-O^{2-}-Mn^{4+},[12–14] which fosters the spin canting and ferromagnetic ordering. Also important are mechanisms such as the electron-electron interaction, and the steric and Jahn-Teller effects.[15] Such a rich mixture of interactions is destined to create some interesting electronic and magnetic states. Indeed, at $x=\frac{1}{3}$ doping, the solid is a ferromagnet (FM) with a large magnetoresistance (MR) associated with the magnetic dynamics near T_c. At another critical doping level, $x=\frac{1}{2}$, which has received much interest lately, even larger MR has been observed as the solid undergoes a first-order field-induced insulator-to-metal transition.[6,8–10] In contrast to $x=\frac{1}{3}$, the magnetotransport in $x=\frac{1}{2}$ is associated with an antiferromagnet (AFM)-to-FM transition. The group at University of Tokyo[8] was the first to interpret the transition as a result of melting of the charge-ordered lattice in $Pr_{0.5}Sr_{0.5}MnO_3$. Later the same group reported a similar transition in $Nd_{0.5}Sr_{0.5}MnO_3$.[9]

In this paper, we report the observation of *four* field-induced electronic states, rather than just two states (insulator and metal), in another half-doped $La_{0.5}Ca_{0.5}MnO_{3+\delta}$ which has the smallest tolerance factor among the solids studied so far.[6,8–10] They are achieved as we change the degree of canting in the AFM state which is eventually driven to an FM state in a large field (H). The first-order phase transitions between the electronic states are accompanied by multiple drops in resistivity ρ, leading to a maximum 10^9-fold change in $\rho(H)$ between the least and the most conducting state. The occurrence of these multiples states may be associated with the unique magnetic structure consisting of an array of one-dimensional (1D) zigzag charge-ordered FM chains with an AFM coupling between them.

The polycrystalline sample of $La_{0.5}Ca_{0.5}MnO_{3+\delta}$ was made with the standard solid-state reaction method (see Ref. 6). The thermal annealing (at $T\approx$1300 C) lasted about eight days to ensure homogeneity. X-ray diffraction patterns confirm a single phase which was indexed based on the manganate structure. No secondary phases were detected in our x-ray system which is capable of 1% impurity detection. The magnetization of the sample was measured in both a superconducting quantum interference device (SQUID) magnetometer and a high-field magnetometer at the MIT Bitter National Magnet Laboratory.

The manganate is a strong magnetoresistive solid. We have measured the magnetoresistance (MR) and magnetization (M) over a wide H range and at various temperatures (T). For each measurement, we cooled the sample to a selected T in *zero field* and then measured $\rho(H)$ and $M(H)$ in a sweeping H (0→19 T→0→−19 T→0→19 T). The results are shown in Fig. 1 for T=4.2, 50, and 77 K. Both MR and M are strongly dependent on the thermal and magnetic history of the sample.

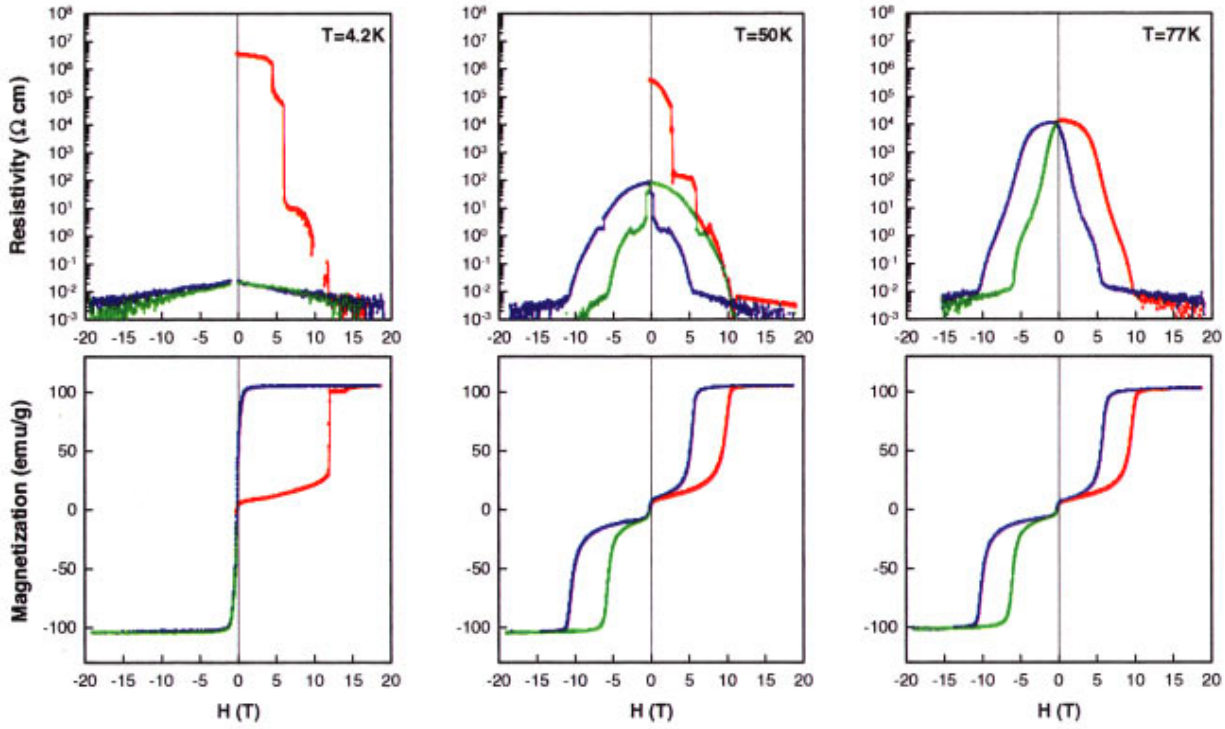

FIG. 1. Resistivity (in log scale) and magnetization of $La_{0.5}Ca_{0.5}MnO_{3+\delta}$ versus magnetic field at $T=4.2$, 50, and 77 K. For each run, the sample was cooled in zero field, and then subjected to a sweeping field sequence: (red) 0→19 T; (blue) 19 T→0→−19 T; (green) −19 T→0→19 T.

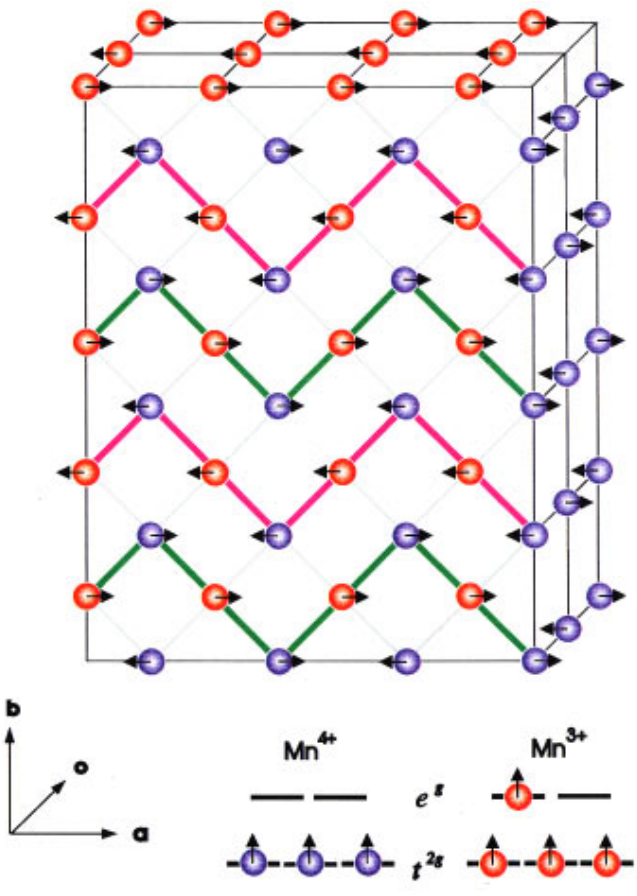

FIG. 2. The charge and spin ordering structure of $La_{0.5}Ca_{0.5}MnO_{3+\delta}$ (a-b plane). Only the Mn^{3+} and Mn^{4+} ions are marked, O^{2-} ions are located midway between the shortest Mn^{3+}-Mn^{4+} pairs. The zigzag chains consist of alternating Mn^{3+} and Mn^{4+} ions whose spins are ordered ferromagnetically. The interchain coupling is of the antiferromagnetic type.

Figure 1 shows that $La_{0.5}Ca_{0.5}MnO_{3+\delta}$ is a metamagnet, which undergoes a transition from AFM to FM and vice versa under a magnetic field or by change of temperature. The low-T ground state is a canted AFM. The extrapolated $M(H\rightarrow 0)$ in the initial state is 5.7% of the fully ordered M (101.5 emu/g) of the FM state. The value of M in the AFM state increases with H as a result of a reduced canting angle. At a sufficiently high H, denoted as $H_c^{A\text{-}F}$, a field-induced first-order phase transition occurs, bringing the system from the AFM to the FM state. Once in the FM state, the system may or may not transform back to the AFM state as $H\rightarrow 0$. At $T=4.2$ K, the system remains in the FM state. However, at an elevated T (e.g., 50 K), the system does collapse back to the AFM state, though at a critical field, $H_c^{F\text{-}A}$, lower than $H_c^{A\text{-}F}$ due to the nature of the first-order transition. The metamagnetism in $La_{0.5}Ca_{0.5}MnO_{3+\delta}$ is similar to earlier results in $Pr_{0.5}Sr_{0.5}MnO_3$ (Ref. 8) and $Nd_{0.5}Sr_{0.5}MnO_3$ (Ref. 9) with one exception, i.e., the induced FM state in other two solids always collapses back to AFM at low field even at 2.5 K. These results point to the existence of an AFM ground state and an FM metastable state. Application of H lowers the total energy of FM due to Zeeman effect, while keeping that of AFM intact. At $H_C^{A\text{-}F}$, the FM state becomes more

stable and an AFM-FM transition appears. If thermal agitation is weak, the system will remain trapped in the metastable FM state even when $H \rightarrow 0$. On the other hand, thermal excitation at a finite T will assist the system to undergo an FM-AFM transition at a lower $H_c^{F\text{-}A}$.

Next we turn our attention to the corresponding changes of MR as the magnetic state evolves in a field. There are three important features in the MR data of Fig. 1. (1) With increasing H, there appear four distinctive electronic states at low T (e.g., 4.2 and 50 K). The zero-field-cooled (ZFC) state at $H_1=0$ and $T=4.2$ K is an insulator with a large ρ of 3.12×10^6 Ω cm. At $H_2=4.52$ T, $H_3=5.98$ T, and $H_4=11.80$ T, three consecutive precipitous drops in ρ cascade the system to three high-H electronic states (we refer to the four states as H_n state with $n=1,2,3,4$). The state H_4 reached at the highest field, which coincides with $H_c^{A\text{-}F}$ of the AFM-FM transition, corresponds to an insulator-to-metal transition. (2) At 4.2 K, once in the trapped FM state, ρ remains at a low value regardless of any subsequent applied field. The maximum change in ρ between the ZFC and the FM state is a dramatic nine orders of magnitude. At a higher T (e.g., 50 K), as $H \rightarrow 0$ from 19 T, ρ undergoes two reversed transitions. One occurs at $H=5.58$ T which corresponds to the FM-AFM transition, and the other at $H=0.30$ T. The ρ at $H=0$ does not revert to the value of the ZFC state, but rather takes the ρ value of the H_2 state. (3) At even higher T (e.g., 77 K), other than the insulator-metal transition at $H=9.85$ T, sharp drops in ρ disappear, indicating that some of the H_n states survive only at low T.

The sharp drops in resistivity in Fig. 1 are intrinsic properties. They are not caused by inhomogeneity or grain boundary effect. The samples used were annealed for an extended period (>1 week) and the x-ray characterization revealed clean and sharp diffraction lines. The largest drop in ρ at H_2 is over four orders of magnitude. It is very unlikely that such a strong effect could result from the grain boundaries in our samples where grain sizes exceed 10 μm. Also the transitions occur consistently on both sides of positive and negative fields (see data at 50 K). Further confirmation of the results using single crystal samples is highly desirable. Unfortunately, single crystals of Ca-doped manganates, unavailable till now, are very difficult to grow.

The microscopic origins of the observed four H_n states are not clear at this stage. They may be due to the unique magnetic structure of $A_{0.5}B_{0.5}MnO_3$, determined by neutron diffraction in the past.[3,16] Figure 2 shows the magnetic structure (a-b plane) at low T, commonly referred to as the CE type,[3,15,16] in which both the charges and the spins of Mn^{3+} and Mn^{4+} (1:1 ratio) are ordered. The e_g^1 electrons in Mn^{3+} ions occupy every other site in the a-b plane. The charge ordering is perfect at exactly $x=\frac{1}{2}$ (half filling). It is noted that the Coulomb interaction in this charge lattice is minimized. The spin ordering of the CE type is such that, along a single zigzag chain (marked in Fig. 2) with alternating Mn^{3+} and Mn^{4+} ions,[3,15,16] the intrachain magnetic moments are ordered ferromagnetically. However all the neighboring chains exhibit AFM ordering. The same is true along the c axis, the neighboring a-b planes have identical charge orderings, except the neighboring chains are ordered antiferromagnetically.

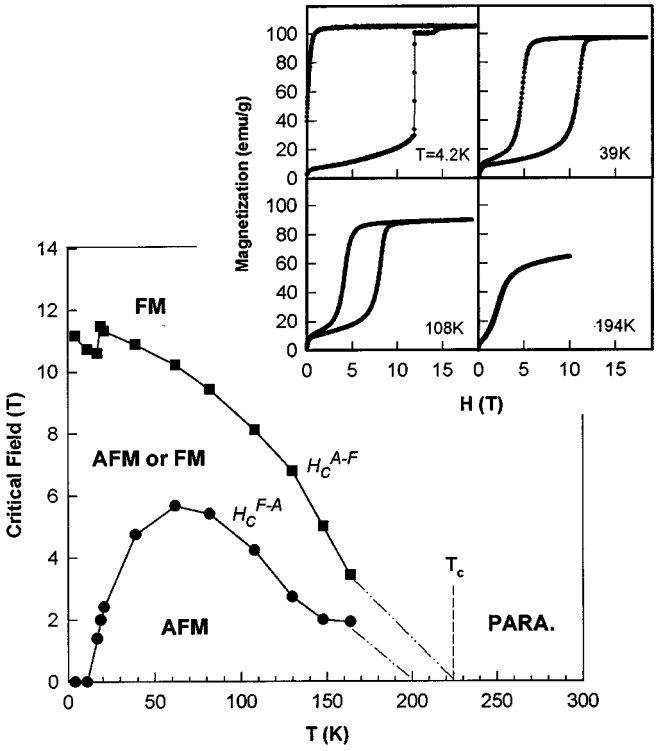

FIG. 3. Phase diagram in the H-T plane. $H_c^{A\text{-}F}$ and $H_c^{F\text{-}A}$ are critical fields for the AFM-FM and FM-AFM transitions respectively. Inset: Magnetization vs field at various temperatures.

Based on the magnetic structure we conjecture a scenario in which transitions among H_n states may occur. The Mn^{4+} content in our sample has been determined to be 53% due to a slight oxygen excess.[6] In other words, 3% of the e_g^1 electrons in the a-b planes are missing, or equivalently there are 3% extra holes in the charge lattice. The double-exchange model predicts that the hopping strength between Mn^{3+} and Mn^{4+} is $t=b\cos(\Theta/2)$, Θ being the angle between the neighboring spins.[13,14] Under normal circumstances, an independent FM zigzag chain would behave like a 1D conductor, because electrons can hop freely. However, in the a-b plane electron hopping along a chain is impeded by the Coulomb repulsion from three neighboring electrons. This is why the solid is an insulator. If a small amount of electrons are removed as in our sample, the electrons in the chains could now tunnel into these electron vacancies (holes) against a reduced Coulomb barrier from two electrons, instead of three. At low T the holes would most likely be trapped. Application of H would reduce the canting angle Θ between the spins on the neighboring chains, enhancing the interchain electron hopping. At H_2, the trapped holes may become delocalized, because the interchain hopping would effectively reduce the Coulomb interaction. The motion of these holes would be confined along the 1D zigzag chains. Further increase in H may introduce a 2D character in the electron conduction by continuously increasing the interchain electron hopping. At H_3 a major drop in ρ sets in, a possible indication of a partial 2D charge-lattice melting. Finally, at the even higher H_4, the AFM-FM transition makes the system a truly 3D conductor, leading to a complete melting of

the charge lattice. We emphasize that the above scenario is just a conjecture. We feel that the 1D FM chains may play some roles in the magnetotransport. Again, single crystals would be desirable in assessing these ideas.

In addition to the aforementioned dramatic H-induced effect, the results in Fig. 1 also convey the significant role of T. We have characterized the thermal effect by measuring $M(H)$ at different temperatures as shown in the inset of Fig. 3. The critical fields, $H_c^{A\text{-}F}$ and $H_c^{F\text{-}A}$, are found to be strongly dependent on T, from which a magnetic phase diagram has been constructed in Fig. 3. With increasing T, it requires smaller field, $H_c^{A\text{-}F}$, to induce the AFM-FM transition. This is understandable because the net energy required for the transition is the sum of the magnetic energy and the thermal energy. Once the system is in the FM state, lowering H to $H_c^{F\text{-}A}$ will bring it back to the AFM state. But at $T<10$ K even at $H=0$, the system remains trapped in the FM state. However, at a higher T, thermal energy destabilizes the FM state. Indeed $H_c^{F\text{-}A}$ starts to increase with increasing T until about $T_p=60$ K. The energy, $k_B T_p \approx 0.52$ meV, is the energy barrier (per spin) that the system must overcome to undergo the FM-AFM transition. We also note that the four H_n states are most pronounced when $T<T_p$ (see Fig. 1), which makes T_p a characteristic energy scale for the physics at low and high T. Figure 3 can also be used as a phase diagram for the electronic states, with the FM and AFM phases corresponding to the metallic and insulating states, respectively. The hysteresis region is the area between the upper and lower curves in Fig. 3. In this region the solid can be either an insulator, if starting from the H_1 state, or a metal, if from the H_4-state.

It is worthwhile to make a comparison among the three half-doped manganates studied so far, $Pr_{0.5}Sr_{0.5}MnO_3$ (Ref. 8), $Nd_{0.5}Sr_{0.5}MnO_3$ (Ref. 9), and $La_{0.5}Ca_{0.5}MnO_3$. Though similar in many aspects, the three solids have major differences in their properties. In the first two (Pr/Sr and Nd/Sr), there exists an insulator-to-metal transition, whereas in La/Ca there are two additional states between the insulating and metallic ends. The hysteresis area in the phase diagram increases in the order of Pr/Sr, Nd/Sr, to La/Ca ($\Delta H_c = H_c^{A\text{-}F} - H_c^{F\text{-}A}$ changes from 1, 9, to 11 T). In particular, the FM state in La/Ca can be trapped up to $T=10$ K once magnetized. However, the FM state is not stable at all in zero field in Pr/Sr and Nd/Sr even down to 2.5 K. These differences may result from the degree of structural distortion in these solids. The buckling distortion of the MnO_6 octahedra depends on the tolerance factor which is a measure of cation size mismatch. The smaller the tolerance factor, the larger the distortion, and the smaller the Mn-O-Mn bond angle in the plane.[11] In the sequence of Pr/Sr, Nd/Sr, and La/Ca, the tolerance factor become increasingly smaller (0.928, 0.925, and 0.909), and so does the e_g electron hopping integral. This is consistent with the fact that the low-T resistivity at zero field increases dramatically from 10^{-2}, 10^2, to 10^6 Ω cm in these solids. Magnetic field, on the other hand, increases electron hopping integral by reducing the canting angle. Therefore in La/Ca a wider range of electron hopping parameter can be accessed in a magnetic field, and this could be a reason why the multiple states are observed in the La/Ca, and not in the Pr/Sr or Nd/Sr solids.

We wish to thank W. J. Gallagher, X. W. Li, J. C. Slonczewski, R. Laibowitz, R. Koch, and D. P. DiVincenzo for stimulating discussions and help. This work was supported by National Science Foundation Grant Nos. DMR-9258306 and DMR-9414160 and IBM.

[1] R. von Helmolt, J. Wecker, B. Holzapfel, L. Schultz, and K. Samwer, Phys. Rev. Lett. **71**, 2331 (1993).
[2] S. Jin, T. H. Tiefel, M. McCormack, R. A. Fastnacht, R. Ramesh, and L. H. Chen, Science **264**, 413 (1994).
[3] E. O. Wollan and W. C. Koehler, Phys. Rev. **100**, 545 (1955).
[4] G. H. Jonker and J. H. van Santen, Physica **16**, 337 (1950).
[5] S. Jin, H. M. O'Bryan, T. H. Tiefel, M. McCormack, and W. W. Phodes, Appl. Phys. Lett. **66**, 382 (1995).
[6] G. Q. Gong, C. L. Canedy, Gang Xiao, J. Z. Sun, A. Gupta, and W. J. Gallagher, Appl. Phys. Lett. **67**, 1783 (1995).
[7] M. F. Hundley, M. Hawley, R. H. Heffner, Q. X. Jia, J. J. Neumeier, J. Tesmer, J. D. Thompson, and X. D. Wu, Appl. Phys. Lett. **67**, 860 (1995).
[8] Y. Tomioka, A. Asamitsu, Y. Moritomo, H. Kuwahara, and Y. Tokura, Phys. Rev. Lett. **74**, 5108 (1995).
[9] H. Kuwahara, Y. Tomioka, A. Asamitsu, Y. Moritomo, and Y. Tokura, Science **270**, 961 (1995).
[10] P. E. Schiffer, A. P. Ramirez, W. Bao, and S-W. Cheong, Phys. Rev. Lett. **75**, 3336 (1995); P. G. Radealli, D. E. Cox, M. Marezio, S-W. Cheong, P. E. Schiffer, and A. P. Ramirez, *ibid.* **75**, 4488 (1995).
[11] H. Y. Hwang, S-W. Cheong, P. G. Radaelli, M. Marezio, and B. Battlog, Phys. Rev. Lett. **75**, 914 (1995).
[12] C. Zener, Phys. Rev. **82**, 403 (1951).
[13] P. W. Anderson and H. Hasegawa, Phys. Rev. **100**, 675 (1955).
[14] P.-G. de Gennes, Phys. Rev. **118**, 141 (1960).
[15] J. B. Goodenough, Phys. Rev. **100**, 564 (1955).
[16] Z. Jirak *et al.*, J. Magn. Magn. Mater. **53**, 153 (1985); K. Knizek, Z. Jirak, E. Pollert, F. Zounova, and S. Vratislav, J. Solid State Chem. **100**, 292 (1992).